

MicroRNA528, a hub regulator modulating ROS homeostasis via targeting of a diverse set of genes encoding copper-containing proteins in monocots

Hong Zhu^{1*} , Chengjie Chen^{2,3*} , Jun Zeng¹ , Ze Yun¹, Yuanlong Liu^{2,3}, Hongxia Qu⁴ , Yueming Jiang⁴ , Xuewu Duan⁴  and Rui Xia^{2,3} 

¹Key Laboratory of South China Agricultural Plant Molecular Analysis and Genetic Improvement, South China Botanical Garden, Chinese Academy of Sciences, Guangzhou 510650, China;

²State Key Laboratory for Conservation and Utilization of Subtropical Agro-Bioresources, College of Horticulture, South China Agricultural University, Guangzhou 510642, China; ³China Key

Laboratory of Biology and Germplasm Enhancement of Horticultural Crops in South China, Ministry of Agriculture, Guangzhou 510642, China; ⁴Key Laboratory of Plant Resources

Conservation and Sustainable Utilization, Guangdong Provincial Key Laboratory of Applied Botany, South China Botanical Garden, Chinese Academy of Sciences, Guangzhou 510650, China

Summary

Authors for correspondence:

Rui Xia

Tel: +86 20 38348652

Email: rxia@scau.edu.cn

Xuewu Duan

Tel: +86 20 37252960

Email: xwduan@scbg.ac.cn

Yueming Jiang

Tel: +86 20 37252525

Email: ymjjiang@scbg.ac.cn

Received: 4 April 2019

Accepted: 13 August 2019

New Phytologist (2020) **225**: 385–399

doi: 10.1111/nph.16130

Key words: banana, evolution, microRNA528, monocot-specific, polyphenol oxidase (*PPO*), reactive oxygen species (ROS) homeostasis.

Introduction

For more than two decades, microRNAs (miRNAs) have been studied widely as important regulatory molecules, involving almost all aspects of the plant life cycle. Plant miRNAs, *c.* 20–22 nt long, are derived from the processing of longer primary *MIRNA* transcripts with hairpin structures (Ramachandran & Chen, 2008). MicroRNAs usually suppress the expression of their target genes by guiding mRNA degradation and/or translational repression via sequence complementarity (Jones-Rhoades *et al.*, 2006; Voinnet, 2009). Although initial studies have largely demonstrated the role of miRNAs in morphogenesis and development processes in plants (Chen, 2012), emerging studies show that plant miRNAs also are essential in stress responses (Sunkar *et al.*, 2012). Of the stress-responsive

- Plant microRNAs (miRNAs) regulate vital cellular processes, including responses to extreme temperatures with which reactive oxygen species (ROS) are often closely associated.
- In the present study, it was found that aberrant temperatures caused extensive changes in abundance to numerous miRNAs in banana fruit, especially the copper (Cu)-associated miRNAs. Among them, miR528 was significantly downregulated under cold stress and it was found to target genes encoding polyphenol oxidase (*PPO*), different from those identified in rice and maize. Expression of *PPO* genes was upregulated by >100-fold in cold conditions, leading to ROS surge and subsequent peel browning of banana fruit.
- Extensive comparative genomic analyses revealed that the monocot-specific miR528 can potentially target a large collection of genes encoding Cu-containing proteins. Most of them are actively involved in cellular ROS metabolism, including not only ROS generating oxidases, but also ROS scavenging enzymes.
- It also was demonstrated that miR528 has evolved a distinct preference of target genes in different monocots, with its target site varying in position among/within gene families, implying a highly dynamic process of target gene diversification. Its broad capacity to target genes encoding Cu-containing protein implicates miR528 as a key regulator for modulating the cellular ROS homeostasis in monocots.

miRNAs reported, there is a specific group initially coined as copper microRNAs (Cu-miRNAs), because they target a number of genes encoding Cu-containing proteins (Burkhead *et al.*, 2009). It is now well known that there are three major types of Cu centers in the Cu-containing proteins (Choi & Davidson, 2011). Type 1 Cu centers (T1) bind a single Cu and proteins of type 1 are relatively small without any other metal or cofactor. These types of Cu-containing proteins are commonly called blue Cu proteins or cupredoxins, which function not as oxidases but rather, primarily as electron transfer proteins; examples include plastocyanin and mavyanin from plants. Type 2 Cu centers (T2) bind Cu in a square planar coordination and usually occur in enzymes to assist oxidizing reactions, as exemplified by Cu/Zn superoxide dismutase (Cu/ZnSOD). Type 3 Cu centers (T3) are binuclear because they bind two Cu atoms and occur in enzymes that are oxidases and oxygenases, and in oxygen-transporting proteins; a typical

*These authors contributed equally to this work.

example is tyrosinase (like polyphenol oxidase, PPO) in plants and fungi. There are some other enzymes that have been characterized to contain multiple type 1, 2 and 3 Cu centers to catalyze reactions, also known as multicopper oxidases or multi-domain cupredoxins (Nakamura & Go, 2005). Among these multicopper oxidases, laccase (LAC) and ascorbate oxidase (AAO) both contain three homologous domains of cupredoxins and are distributed widely in fungi and higher plants. Copper-containing proteins are of diverse functions that are critical for stress responses (Choi & Davidson, 2011).

The first well-characterized Cu-miRNA is miR398 in *Arabidopsis*, targeting several well-known stress-responsive genes (i.e. Cu/Zn superoxide dismutases genes (*CSD1* and *CSD2*)) in the context of oxidative stress protection (Sunkar *et al.*, 2006; Yamasaki *et al.*, 2007; Dugas & Bartel, 2008). miR397, miR408 and miR857 also have been reported to target genes encoding Cu-containing proteins plantacyanin and laccase (Abdel-Ghany & Pilon, 2008). These Cu-miRNAs are largely conserved from mosses to conifers and angiosperms; they accumulate at low Cu concentrations and disappear at sufficiently high Cu concentrations (Yamasaki *et al.*, 2007; Abdel-Ghany & Pilon, 2008). In addition, several species- or lineage-specific miRNAs identified from different plant species belong to this group. These include miR528 in rice and maize, miR1073 in moss and miR1444 in poplar (Lu *et al.*, 2011; Higashi *et al.*, 2013; Wu *et al.*, 2017; Sun *et al.*, 2018). miR528 has been reported to be involved in multiple plant stress responses (Li *et al.*, 2013; Chavez-Hernandez *et al.*, 2015; Sharma *et al.*, 2015; Ragupathy *et al.*, 2016). In rice, miR528 has been validated to target at least four mRNA transcripts, encoding two plastocyanin-like proteins, an L-ascorbate oxidase, and an EIN3-binding F-box protein, respectively (Zhou *et al.*, 2010; Li *et al.*, 2011; Wu *et al.*, 2017). Some of these targets have been characterized as involved in multiple biological events, particularly in redox processes. For example, the target gene for EIN3-binding F-box protein (*D3*) has been reported as a positive regulator in the hydrogen peroxide-induced cell death (Yan *et al.*, 2007). Another study in rice shows that upon virus infection, miR528 becomes preferentially associated with AGO18, which leads to higher AAO activity and reactive oxygen species (ROS) concentration, and thus enhanced antiviral resistance (Wu *et al.*, 2017). In creeping bentgrass, constitutive expression of rice miR528 can enhance the tolerance to salinity stress and N starvation by repressing *AAO* and *CBP1* (Cu ion binding protein 1) transcripts (Yuan *et al.*, 2015). A recent study further demonstrates that if maize plants are exposed to excessive nitrogen supply, miR528 accumulates to downregulate its *LAC* targets, resulting in reduced lignin content and lodging resistance (Sun *et al.*, 2018).

Temperature stresses, including both cold and heat, adversely affect plant growth and development, as well as the postharvest life and quality of fruits and vegetables (Wahid *et al.*, 2007; Knight & Knight, 2012). Banana (*Musa acuminata*) is a major tropical crop and one of the most popular fruits worldwide. As an important component of daily diet of people, a year-round supply of banana requires storage at relatively low temperature to minimize metabolic activity and maximize the shelf life of the

fruit. However, banana fruit are sensitive to temperature fluctuation. On the one hand, when the fruit are exposed to low temperatures of <12°C, the peel turns gray and browning progresses quickly; fruit ripening stalls with the pulp hardening, leading to serious economic losses. On the other hand, when fruit are kept at high temperatures, quick fruit softening occurs with the peel staying green. Therefore, temperatures between 13 and 15°C are usually the best for postharvest storage and long-distance transportation for banana, but it is costly and technically difficult to maintain these storage conditions in commercial practice. Previous studies suggest that the peel browning of banana fruit under low-temperature storage is caused mainly by PPOs, and the main substrates are tannin and dopamine (Unal, 2005). PPOs catalyze the oxidation of monophenols and/or o-diphenols to highly reactive o-quinones, which in turn interact with oxygen and proteins to generate ROS and typical brown-pigmented complexes (Steffens *et al.*, 1994). The generation of ROS has been considered as one of the most common plant responses to different stresses (Orozco-Cardenas & Ryan, 1999; Kovtun *et al.*, 2000; Kotchoni & Gachomo, 2006; Mittler *et al.*, 2011; Petrov & Van Breusegem, 2012; Noctor *et al.*, 2014; Xia *et al.*, 2015). Under natural growth conditions, plant adaptations minimize the damage that could be induced by ROS. However, oxygen toxicity appears when ROS production exceeds the quenching capacity of the protective systems due to stress conditions (Miller *et al.*, 2009; Akter *et al.*, 2015). To cope with excessive ROS generated under stress conditions, plants have evolved antioxidant mechanisms involving antioxidant enzymes and nonenzymatic molecules (Mittler, 2002). The former includes superoxide dismutase (SOD), catalase (CAT) and peroxidase (POD), and the later contains mainly glutathione and ascorbate, which can be oxidized to dehydroascorbate via the catalyzation of AAO. These ROS-related enzymes, including PPO, SOD, POD and AAO, are all Cu-containing proteins.

The present study aimed to investigate the roles of miRNAs of banana in response to temperature stresses. The temperature-responsive miRNAs and their targets in banana were comprehensively profiled, revealing that miR528, by targeting *PPO* genes, plays a vital role in the peel browning of cold-stressed banana. Comparative genomic analysis showed that miR528, as a monocot-specific miRNA, likely emerged in Alismatales, and has evolved with different target preferences among different monocot plants. Interestingly, most of these miR528 target genes belong to the class of genes encoding the Cu-containing proteins, which are important for the ROS homeostasis in cells. The present results reveal a dynamic history of the evolution of miR528 target genes and demonstrate its central role in the maintenance of ROS homeostasis in monocots.

Materials and Methods

Plant material and temperature stress treatments

Mature-green 'Brazil' banana fruit (*Musa* spp. AAA group) were harvested from a plantation located in Gaozhou County, Guangdong province for sample collection. Fruit were harvested at 80%

maturity and selected for uniformity and free of defects. All fruit were soaked in 0.2% (w/v) Sporogon solution (Bayer, Leverkusen, Germany) for 3 min to eliminate potential microbes and then air-dried. Three temperatures were set in this study: control at 23°C, cold stress temperature at 6°C and heat stress temperature at 35°C. For each temperature treatment, 90 fruit fingers were selected, packed in 0.02-mm-thick polyethylene bags, and divided into three groups of 30 fingers each as biological replicates. For each replicate sampling, peel tissues (*c.* 50 g) were collected at 2, 4, 5, 6, 8 d from the middle part of three fruit fingers, immediately frozen in liquid nitrogen, and stored at -80°C until use. Sample at 0 d was used as the starting point (before treatment) and shared by treatments.

Measurement of fruit color and firmness under temperature stress

Fruit were monitored every day from 0 d onwards, with representative fruit photographed and compared between control and temperature stress treatments. Peel color was measured by a Minolta Chroma Meter CR-400 (Minolta Camera Co. Ltd., Osaka, Japan). Three fruit fingers were chosen randomly from each treatment at 0 and 5 d. Three equidistant points around the middle position of the surface were taken for color measurement. Three color scales of L*, a* and b* were recorded, where L indicates the lightness or darkness, a* represents green to red and b* denotes blue to yellow. The L scale was used to quantify the change of the peel color under temperature stress.

Fruit firmness was measured by a penetrometer (Model GY-3, Zhejiang Scientific Instruments, Zhejiang, China) with a probe of 0.6 cm in diameter. Three fruit fingers were chosen randomly from each treatment at 0 and 5 d. Each finger was measured at three equidistant points around the middle position of the fruit. The force required to penetrate into the fruit was recorded and expressed in newtons (N).

RNA preparation, deep sequencing and data analysis

Peel samples from control, cold- and heat-stressed fruits were collected at 5 d of storage. Two replicates of total RNA from different samples were extracted using the Plant RNA Purification Reagent (Invitrogen). The quantity and quality of the sRNA were evaluated by Agilent 2100 Bioanalyzer. RNA samples with RNA integrity number (RIN) >8 were sent to LC Sciences (Hangzhou, China) for sRNA sequencing. Approximately 20 µg of mixed RNAs, with equal amounts from all banana peel samples were used for degradome sequencing, a high-throughput sequencing technique used for sRNA target identification. The standard protocol on Illumina HiSeq2000/2500 platform was utilized. All of the sequencing data were first processed by removing the 3' adaptor sequence. Reads homologous to noncoding RNAs and conserved miRNAs were identified by BLASTN alignment against RFAM v.12 and mature miRNA sequences deposited in miRBase 21, allowing up to one mismatch. The total number of reads perfectly matching the banana genome in a given library was used for the normalization of read abundance, which was

denoted as RPM (reads per million genome-matched reads). Banana genome sequences were retrieved from the Banana Genome Hub (*Musa acuminata* DH-Pahang v.2, <http://banana-genome-hub.southgreen.fr>). For degradome data, after adaptor-trimming and genomic mapping, CLEAVELAND 4.4 was optimized to analyze the degradome data. The *P*-value threshold was set to 0.05, and reads at the cleavage site were normalized to transcripts per billion (TPB). To identify differentially expressed miRNAs under temperature stresses, the miRNA expression based on normalized deep-sequencing counts was analyzed by Student's *t*-test based on the experimental design. The significance threshold was set at *P* < 0.01 with fold-changes (stress reads/control reads) > 1.5-fold for identifying differentially expressed miRNAs upon cold or heat stress. All sequencing data are deposited in Gene Expression Omnibus GSE77590.

Assessment of PPO activity and ROS production

Banana peel samples collected on 0, 2, 4, 6 and 8 d were used for the measurement of polyphenol oxidase (PPO) enzymatic activity and reactive oxygen species (ROS) concentration. In brief, 4 g of the sample was ground in 5 ml 0.2 mol l⁻¹ sodium phosphate buffer (pH 6.8) and 0.4 g of PVP on ice. After centrifugation at 15 000 g for 15 min at 4°C, the supernatant was collected as the enzyme extract, and then a 0.1-ml aliquot was diluted into 3 ml reaction system with 2.9 ml 0.01 mol l⁻¹ catechol in 0.2 mol l⁻¹ sodium phosphate buffer (pH 6.8). The absorbance change at 398 nm was measured spectrophotometrically within 10 min. The increased absorbance of 0.01 per min at 398 nm was defined as one unit of PPO activity, expressed as U g⁻¹ FW. The concentrations of ROS species including hydrogen peroxide (H₂O₂), superoxide anion (O₂⁻) and hydroxyl radical (·OH), were determined using assay kits (Suzhou Comin Biotechnology Co, Ltd., Suzhou, China; Nanjing Jiancheng Biochemical Reagent Co, Nanjing, China) in accordance with manufacturer's instructions. H₂O₂ and titanium sulfate can form a yellow titanium peroxide complex with a characteristic absorption peak at 415 nm. O₂⁻ reacts with hydroxylamine hydrochloride to form NO₂⁻, which, under the action of p-aminobenzene sulfonic acid and α-naphthylamine, produces red azo compound with a characteristic absorption peak at 530 nm. ·OH can form a red compound after giving electrons, with a characteristic absorption peak at 550 nm. The activity of other redox-related enzymes including superoxide dismutase (SOD), peroxidase (POD) and ascorbate oxidase (AAO) also was measured using kits (Suzhou Comin Biotechnology) according to the manufacturer's instructions. For each treatment, the measurement was repeated independently three times.

Malondialdehyde (MDA) measurement

One gram of peel tissue sample was homogenized in 8 ml of 10% trichloroacetic acid and then centrifuged at 10 000 g for 10 min. The supernatant was collected and 2 ml was mixed with 2 ml of 0.6% thiobarbituric acid. Two milliliters of distilled water was used as control. The mixture was heated to 100°C for 20 min, quickly cooled to 4°C and centrifuged at

10 000 *g* for 10 min. Absorbance of the supernatant was measured at 532, 600 and 450 nm using a UV spectrophotometer. MDA concentration was calculated according to the formula: $6.45 \times (OD_{532} - OD_{600}) - 0.56 \times OD_{450}$. Three replicates were performed for each measurement.

RNA gel blot

Total RNA was extracted from peel samples of control, cold- and heat-stressed fruit with Plant RNA Isolation Reagent[®] (Invitrogen). For gel blotting, 20 µg of total RNA from banana peel samples was separated on a 15% denaturing polyacrylamide gel and transferred to Amersham Hybond[™]-NX membranes (GE Healthcare, Waukesha, WI, USA). RNA was crosslinked using UV light. The probes of 21–22-nt DNA oligonucleotides reverse-complementary to banana miRNA candidates (Supporting information Table S1) were labeled using a Biotin 3' End DNA Labeling Kit (no. 89818, ThermoFisher). Blots also were probed with a DNA probe complementary to U6 to confirm uniform loading. The prepared membrane filters were hybridized at 37°C overnight, and washed three times at 37°C with stringent washing buffer containing 1 × SSC and 1% SDS. Using Chemiluminescent Nucleic Acid Detection Module (no. 89880; ThermoFisher), membranes were blocked, washed, chromogenically reacted and then exposed to X-ray film for an adjustable time period ranging from 15 min to 2 h, depending on the signal intensity. The blot experiment was performed twice, yielding with similar results.

RLM-5'-RACE

Following the manufacturer's instructions for the FirstChoice RLM-RACE Kit (no. AM1700; Invitrogen), 5 µg of mixed total RNA isolated from banana peel samples was used for ligating 5' RNA adaptors at 37°C for 1 h before reverse transcription at 42°C for 1 h. Gene-specific primers were designed to conduct nested PCRs (Table S1), and PCR products were gel-purified, cloned into the pGM-18T vector (TaKaRa, Dalian, China) and sequenced.

Quantitative real-time PCR

Quantitative real-time (qRT-)PCR was carried out using the same RNA samples used for the gel blot analysis. Total RNA (1 µg) was treated with DNase I and reverse-transcribed with PrimeScript[™] RT reagent Kit (TaKaRa), according to the manufacturer's instructions, using specific stem-loop RT primers for miRNAs and oligo-dT primer for target mRNAs (Table S1). Real-time PCR analysis was carried out using SYBR[®] Premix Ex Taq[™] II (TaKaRa) on an ABI 7500 PCR System (Applied Biosystems, Waltham, MA, USA), according to the standard protocol. The analysis was performed using three independent cDNA preparations and triplicate PCR reactions. The relative expression of miRNAs and target mRNAs was calculated using the $2^{-\Delta\Delta C_t}$ method. Banana 5s rRNA and *Actin* were used as the internal references.

Transient co-expression of *mac-MIR528* and *MaPPO* in *Nicotiana benthamiana* leaves

Constructs harboring *mac-MIR528* primary transcript and *MaPPO1* CDS were prepared separately and transformed into *A. tumefaciens* strain GV3101 (Table S1). Positive transformants were selected (kanamycin and spectinomycin) and target inserts were confirmed by sequencing the PCR products. Around one-month-old *N. benthamiana* plants grown under normal conditions were used for infiltration. Two days pre-infiltration, 2 ml cultures of the *Agrobacterium* strains were inoculated from single colonies on plates and grown for 24 h at 28°C. The working cultures were inoculated from the starter culture at a 1 : 1000 ratio. Cells were harvested by centrifugation at 3000 *g* for 5 min. Cell pellets were resuspended in infiltration medium (10 mM MES, pH 5.7, 10 mM MgCl₂ and 150 mM acetosyringone) with OD₆₀₀ adjusted to 0.5. For co-expression analysis, equal volumes of *Agrobacterium* culture containing *mac-MIR528* and *MaPPO1* were mixed before infiltration. Leaf discs were collected 16, 24 and 40 h post-infiltration and used for RNA extraction and gel blot.

Comparative genomic analysis

Genome sequences and annotations were collected from Phytozome or NCBI GenBank. For species without available genome sequences, transcripts from OneKP were downloaded (Matasci *et al.*, 2014). All protein domains were annotated by NCBI CDD-batch search. Conservation of miR528 precursors was presented using Circos according to the method from (Chorostecki *et al.*, 2017). Syntenic relationships among species were analyzed using MCScanX and visualized by TBTOOLS (Chen *et al.*, 2018a). The un-rooted tree of laccases was reconstructed with RAXML with default settings (Stamatakis, 2014). TBTOOLS also was used for the preparation of a gene ontology (GO) plot, miRNA target gene prediction, the visualization of protein domains, gene structures, miRNA target site distribution, and the plotting of heatmaps and syntenic blocks.

Results

MicroRNAs responded to temperature stresses in banana

Due to its tropical origin, banana fruit is very sensitive to temperature and usually exhibits distinctive injury symptoms under temperature stresses. Particularly under cold treatment (6°C), the peel browning became very serious as soon as 5 d after storage commencement (Fig. 1a), with a significant reduction in the peel lightness (Figs 1b, S1A). Within such a short period of time, however, both control (23°C) and heat-treated (35°C) fruit did not display any visible symptoms, although heat stress caused a sharp drop in the pulp firmness and suppression of fruit yellowing at 5 d (Fig. 1b). To investigate the role of banana miRNAs in response to temperature stresses, banana peel samples were collected at 5 d when both chilling injury and stay-green symptoms were clearly observed (Figs 1a, S1A), and used for sRNA

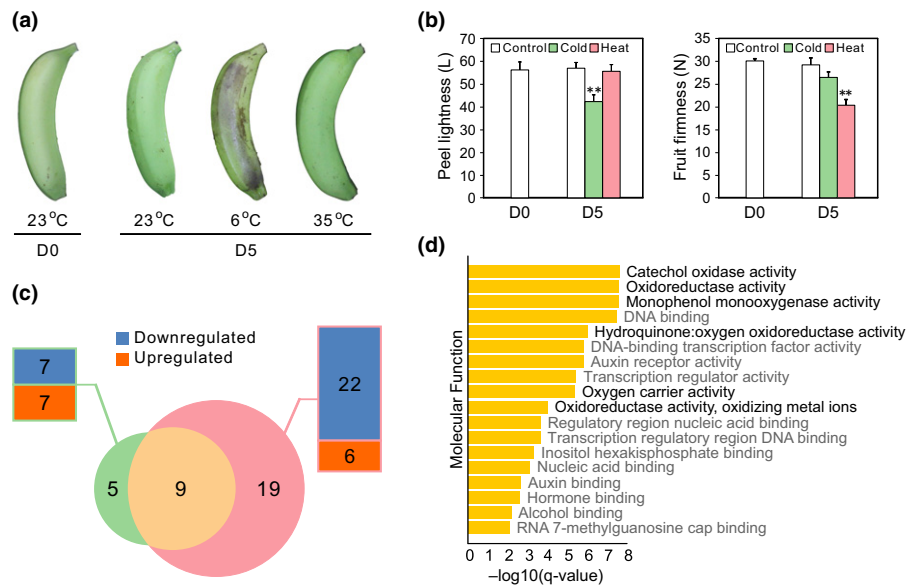


Fig. 1 MicroRNA (miRNA)-mediated regulatory networks in banana fruit in response to temperature stresses. (a) Banana (*Musa acuminata*) fruit display significant appearance and physiological changes under different temperatures. Fruit are kept at 23°C (control), 6°C (cold) and 35°C (heat), respectively. Temperature experiments were performed three times independently with similar results. Representative fruits were photographed and compared before storage (D0) and 5 d after storage (D5) under different temperatures. (b) Measurement of fruit color and firmness of the control, cold- and heat-stressed fruits at D0 and D5, respectively. Each bar indicates the mean \pm SE of triplicate assays and asterisks indicate significant differences between control and temperature-stressed samples (*, $P < 0.05$; **, $P < 0.01$). (c) Differentially expressed banana miRNAs in response to cold or heat stress. The Venn diagram shows the number of common and temperature-specific miRNAs. The bar graphs further present the number and expression trend of differential miRNAs responding to temperature stresses. (d) Enrichment analysis of GO term of all target genes for the temperature-responsive miRNAs in banana. The $-\log_{10}(q\text{-value})$ of enriched gene ontology (GO) terms in molecular function is presented in a descending manner.

sequencing. Analysis of sRNA-sequencing data revealed that both cold and heat stress caused alterations of banana miRNA repertoire in the peel. In total, 14 cold-responsive and 28 heat-responsive miRNAs were identified (Table S2). Nine miRNAs responded to both temperature stresses whereas others showed stress-specific response (Fig. 1c). Equal numbers of miRNAs were upregulated and downregulated by cold. Comparatively, the miRNAs downregulated by heat were almost four times the upregulated ones (Fig. 1c). In the overlapping group of nine miRNAs, four showed the same responsiveness to both temperature stresses whereas the other five miRNAs displayed the opposite responsiveness (Table S2). In the group of the same responsiveness, only one banana-specific miRNA (*mac-miRN3*) was induced but other miRNAs, including *miR167b*, *miR168b/c* and *miR398*, all were suppressed. In the opposite group, *miR396c/d*, *miR396e/f* and *miR529c* were upregulated by cold but downregulated by heat; however, *miR164a/b* and *miR528* were down- and upregulated by cold and heat, respectively (Fig. S1B). Differential expression of these miRNAs based on sRNA sequencing data was largely validated by the results of qRT-PCR and Northern blotting (Fig. S1C).

Next, to investigate the regulatory networks associated with these temperature-responsive miRNAs, their target genes were computationally predicted (Table S3), and subsequently used for GO term enrichment analysis. All target genes were assigned to each term of the Gene Ontology database, and significantly enriched GO terms were found compared to the genome background, taking the corrected $q\text{-value}$ (< 0.01) as a threshold. The

result showed that among the GO terms of molecular function, the categories of oxidase activities (catechol oxidase, oxidoreductase activity and monophenol monooxygenase activity) were most significantly enriched with the top three lowest $q\text{-values}$. Another enriched term was the oxygen carrier activity, which also is associated with the oxidation-reduction process within cells. These results indicate that the oxidation-reduction process of banana fruit is substantially modulated via miRNA pathways in response to temperature stresses (Fig. 1d).

Copper miRNAs play a dominant role in temperature stresses in banana

Of the over-represented oxidation-reduction function categories, a group of genes that encode redox-related proteins were identified, including multicopper oxidase, POD, PPO, LAC, aldehyde oxidase, cysteine oxidase, copper/zinc superoxide dismutase and NADPH-cytochrome P450 reductase. To confirm the involvement of these genes in the temperature stress response of banana, their expression levels were examined under cold and heat treatment. Of the 40 genes tested, most showed undetectable or very low expression whereas only four redox-related genes actively responded to different temperature stresses (Figs 2a, S3B). A *PPO* gene (*Ma08_t34740*) and a *LAC* gene (*Ma09_t17350*) were significantly induced by cold (6°C) but suppressed by heat (35°C); the cold treatment dramatically promoted the expression of the *PPO* gene with an increase of up to *c.* 150-folds (Fig. 2a). A *Cu/ZnSOD* gene (*Ma02_t04310*) was upregulated in the cold-

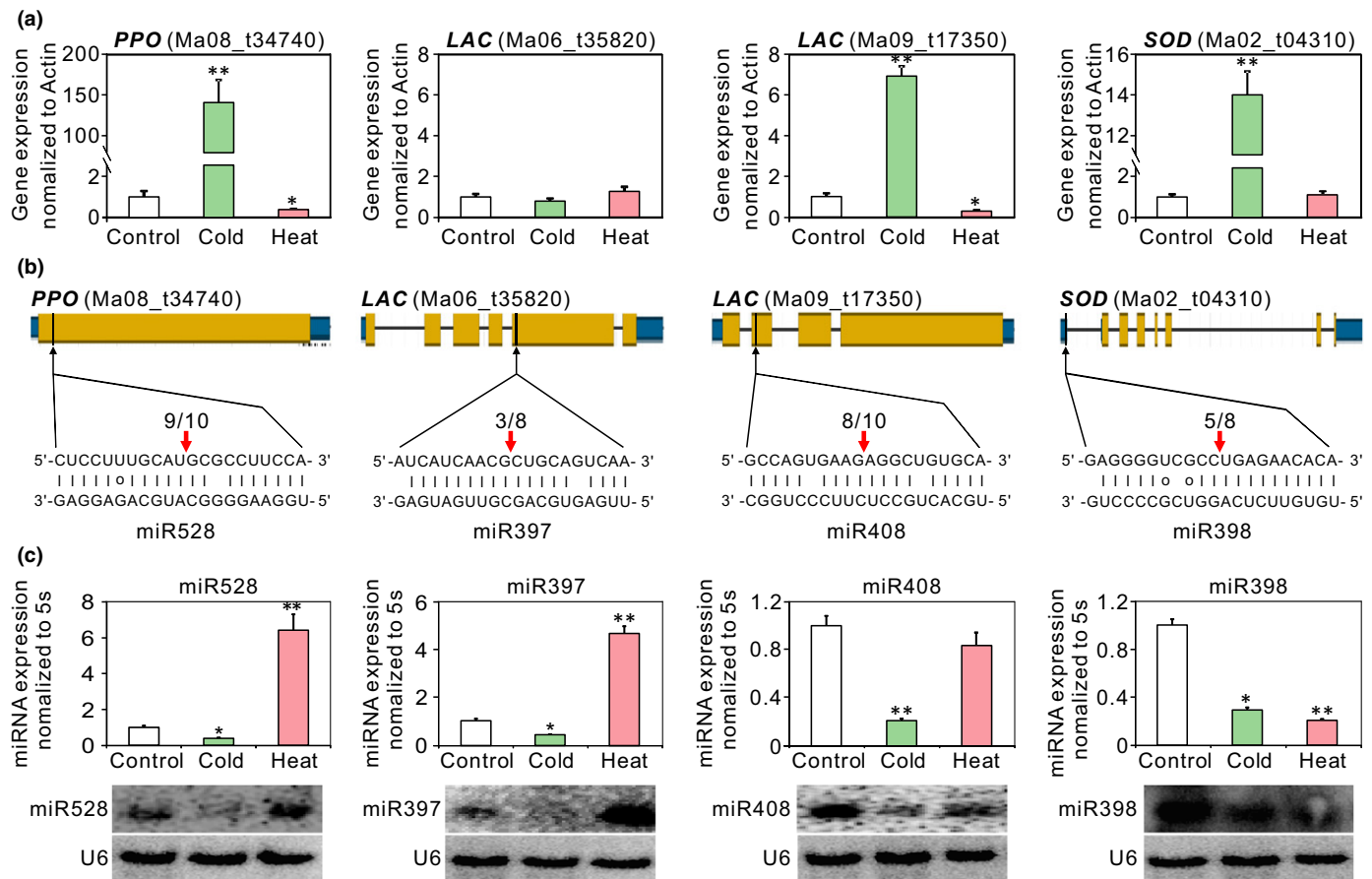


Fig. 2 Redox-related genes are jointly regulated by microRNA (miRNA) in banana temperature stress response. (a) Quantitative expression analysis of multiple redox-related genes from the most enriched gene ontology (GO) categories in Fig. 1(d). The expression level of the genes in the control fruit sampled at 5 d is set as 1. Banana (*Musa acuminata*) *Actin* gene is used as internal control. Each bar indicates the mean \pm SE of triplicate assays and asterisks indicate significant differences in expression between control and temperature-stressed samples (*, $P < 0.05$; **, $P < 0.01$). (b) Alignments of copper-miRNAs miR528, miR397, miR408 and miR398 with their corresponding redox-related gene targets validated in banana. Arrows indicate the cleavage sites of target mRNAs, as detected with the 5'-RACE assay and the fractions above the red arrows show the numbers of clones with an identified 5' end detected in the total sequenced clones. (c) Quantitative expression analysis of miR528, miR397, miR408 and miR398, as determined via stem-loop quantitative real-time (qRT)-PCR and RNA gel blot, respectively. The expression level of the miRNAs in the control fruit sampled at 5 d was set as 1. Banana 5s rRNA and U6 sequences were used as controls. Each bar indicates the mean \pm SE of triplicate assays and asterisks indicate significant differences in expression between control and temperature-stressed samples (*, $P < 0.05$; **, $P < 0.01$).

stressed sample, with little change in the heat treatment (Fig. 2a). In combination with the data herein from degradome sequencing (Table S3), these three genes were found to be targeted by miR528, miR397/miR408 and miR398 in banana, respectively. Another *LAC* gene (Ma06_t35820) targeted by miR397 had very low expression and responsiveness to stress temperatures (Fig. 2a, b). A few of these targeting relationships were further experimentally validated by analysis of uncapped mRNA fragments (RLM-5'-RACE) (Figs 2b, S2). All these four miRNAs showed responsiveness to at least one temperature stress (Table S2; Fig. S1B), and further examination of their expression patterns via stem-loop qRT-PCR and RNA gel blot confirmed that the expression of these miRNAs was inversely correlated with their target expression (Fig. 2c). Specifically, the expression pattern of miR528 and miR397 was quite similar – both miRNAs were downregulated by cold and upregulated by heat. By contrast, both cold and heat caused reduced expression of miR408 and miR398 to various

degrees (Fig. 2c). These temperature-responsive miRNAs have been recently referred to as Cu-miRNAs, as they are widely present in plants and play an important role in regulating Cu-containing proteins, which function as electron transfer shuttles to mediate the oxidoreduction between proteins (Burkhead *et al.*, 2009; Pilon, 2017). The results herein have demonstrated the active involvement of these Cu-miRNAs in the temperature response in banana.

Banana miR528 targets genuine *PPO* genes that are critical for fruit ROS state and peel browning

In order to confirm the regulation of miR528 on *PPO* genes, *in vivo* validation was conducted by infiltrating *Agrobacterium* harboring *mac-MIR528* primary transcript and *MaPPO1* into *N. benthamiana* leaves for transient co-expression analysis. As expected, miR528 accumulation was much higher in leaves

infiltrated with miR528, or miR528 + *MaPPO1* constructs relative to the *MaPPO1*-infiltrated leaves, with the *MaPPO1* transcript being detected only in samples infiltrated with *MaPPO1* or *MaPPO1* + miR528 constructs (Fig. 3a). The *MaPPO1* level was substantially reduced in the leaves when miR528 and *MaPPO1* were co-expressed, compared to the level in leaves where *MaPPO1* was expressed alone (Fig. 3a). Therefore, *PPO* genes were a class of genuine target genes for miR528 in banana.

In order to further investigate the role of Cu-miRNAs under different temperature stresses in banana fruit, their expression was monitored over a longer period, during which the fruit gradually and progressively reacted with related symptoms (Fig. S1A). The time-course RNA blots of the above-mentioned Cu-miRNAs further revealed that all, in particular miR528, were gradually suppressed upon cold stress, whereas miR528 and miR397 were induced, especially later, by heat stress (Fig. 3b). Stem-loop qRT-PCR assay further confirmed the expression

trend of these miRNAs (Fig. S3A). The substantial downregulation of miR528 and the extraordinary increase of its target *PPO* gene (Fig. 2) suggested its further analysis. There are seven *PPO* genes encoded in the banana genome, and expression of five *PPO* genes was detectable (Figs 3c, S3B), with three of them (referred as *MaPPO1/2/3*) showing significant expression changes under temperature stresses (Fig. 3c). Interestingly, all of these three *PPO* genes possess a canonical miR528 target site, and the miR528-directed cleavage was validated in two of them (*MaPPO1* and *MaPPO3*; Table S3; Fig. S2). *MaPPO1/2/3* showed a clear opposite expression trend to that of miR528, especially for *MaPPO1* and *MaPPO2*, for which expression surged hundreds of times greater in cold treatment but diminished to very low level upon heat treatment (Fig. 3b,c).

Next, to evaluate the fruit ROS state, PPO activity was assayed under different temperature stresses. As expected, the PPO activity started to increase from 2 d after the fruit were subjected to

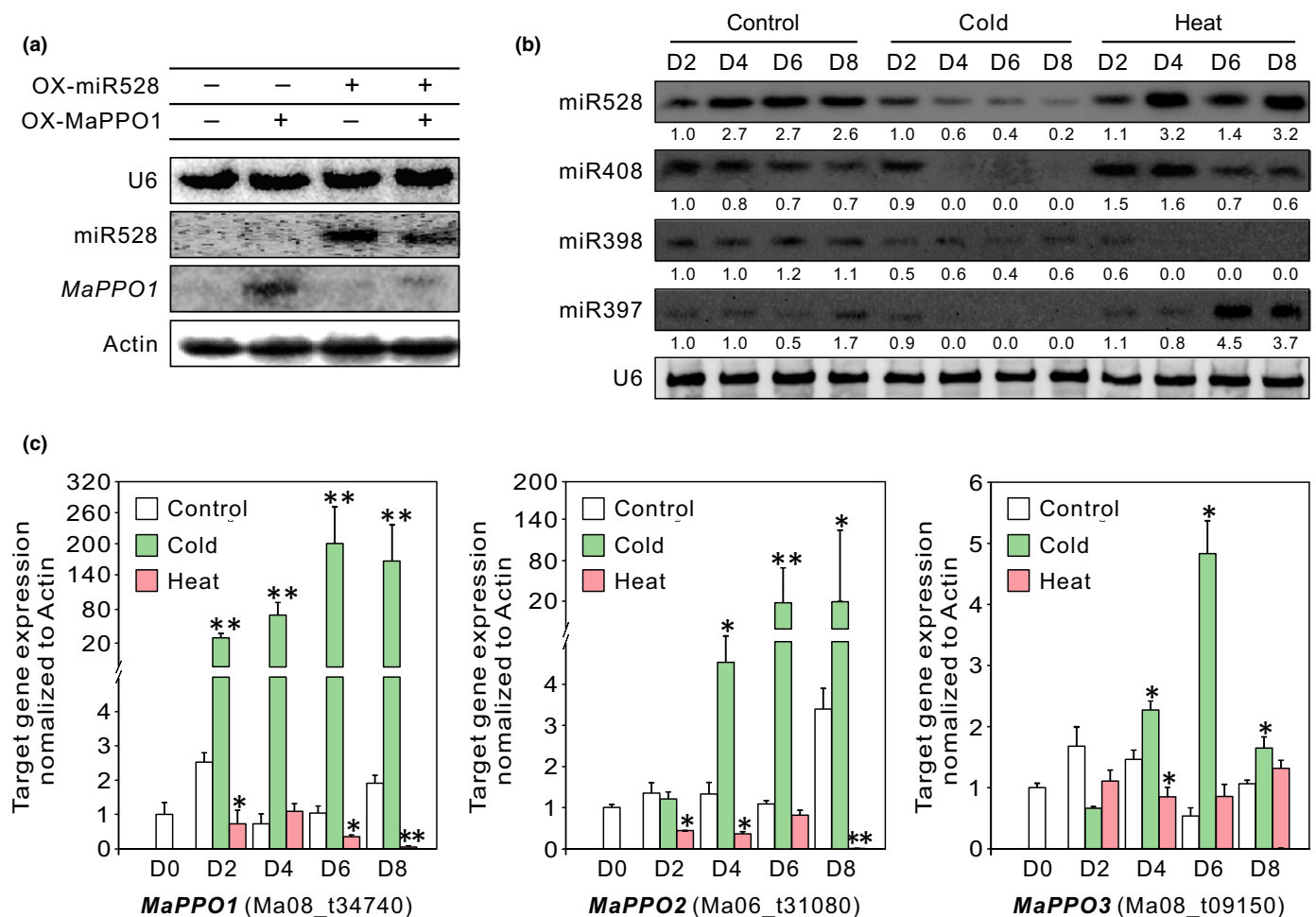


Fig. 3 The microRNA (miR)528-*PPO* module in banana temperature stress response. (a) Accumulation of the indicated targets after transient co-expression analysis of *mac-MIR528* and *MaPPO1* transcripts in *Nicotiana benthamiana* leaves. Vectors used in each lane are shown in the upper table. Banana (*Musa acuminata*) U6 and *Actin* sequences were used as controls. (b) Time-course expression patterns of miR528, miR397, miR408 and miR398 in banana under temperature stresses via RNA gel blot. Banana U6 was used as a loading control. Numbers below the bands are the expression values of the samples relative to those of U6, calculated by the IMAGE software. (c) Time-course expression patterns of three *PPO* targets (*MaPPO1-3*) of miR528 under temperature stresses. The expression level of the genes in the control fruit sampled at 0 d is set as 1. Banana *Actin* was used as a control. Bar values are the means \pm SEs of triplicate assays and asterisks indicate significant differences in expression between control and temperature-stressed samples at each time point (*, $P < 0.05$; **, $P < 0.01$). *PPO*, polyphenol oxidase.

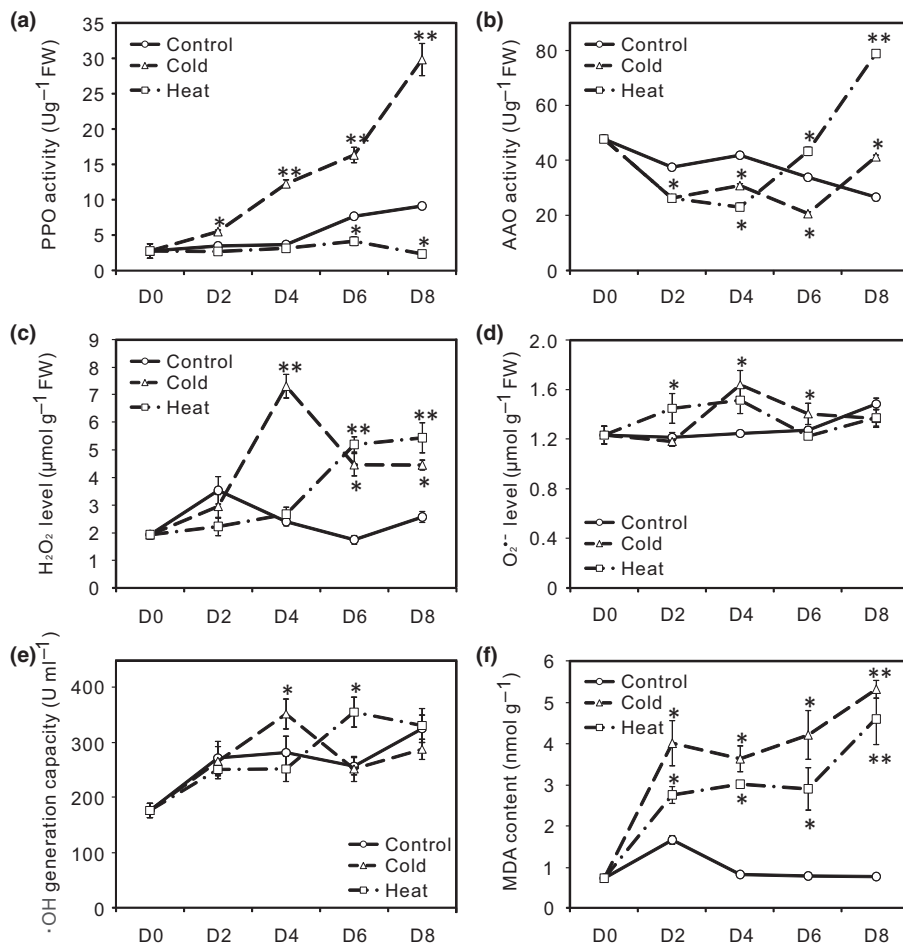


Fig. 4 Changes of redox-related enzyme activity and fruit reactive oxygen species (ROS) state in banana peel. (a, b) Time-course changes of PPO and AAO enzymatic activity under temperature stresses. Data points are the means \pm SE of triplicate assays and asterisks indicate significant differences in enzyme activity between control and temperature-stressed samples at each time point (*, $P < 0.05$; **, $P < 0.01$). (c–e) Time-course changes of ROS components, including H_2O_2 , $O_2^{\cdot-}$ and $\cdot OH$ under temperature stress. (f) Time-course change of malondialdehyde (MDA) level under temperature stress. Data points are the means \pm SE of triplicate assays and asterisks indicate significant differences between control and temperature-stressed samples at each time point (*, $P < 0.05$; **, $P < 0.01$).

cold and remained at a higher level compared to the control (Fig. 4a). Conversely, PPO activity was largely suppressed at minimum level in the heat-stressed fruit, especially at later stages (Fig. 4a). Correspondingly, brown spots gradually were observed in the peel of cold-stressed fruit after 2 d, whereas the color remained almost unchanged for the heat-stressed fruit (Fig. S1A). The enzyme activity of AAO also was measured, but unlike that of PPO, it was lower under cold and heat stress than the control group in the first 4–6 d. Afterwards, the AAO enzyme activity gradually increased and became higher than the control, especially in the heat-stressed fruit (Fig. 4b). In plants, PPOs are actively involved in oxidative process, generating ROS. The burst of PPO activity resulted from reduced miR528 level under cold stress may link with the enhancement of ROS production. Therefore, measurements were made of the ROS concentrations, mainly represented by H_2O_2 , $\cdot OH$ and $O_2^{\cdot-}$, in the temperature-stressed banana peel (Fig. 4c–e). It was found that there was a very significant H_2O_2 burst after 4 d in the cold-stressed fruit, and the H_2O_2 concentration remained higher than the control afterwards (Fig. 4c). Similar results were observed for $O_2^{\cdot-}$ and $\cdot OH$ in the cold-stressed fruit, where both components also showed a significant increase at 4 d (Fig. 4d,e). For the heat-stressed fruit, the concentration of $O_2^{\cdot-}$ appeared to increase in the early stage, whereas both H_2O_2 and $\cdot OH$ also were induced

but at a later stage, likely through activities other than that of PPOs (Fig. 4c–e). As the direct product and indicator of membrane peroxidation, MDA level increased significantly in both cold- and heat-stressed fruit, especially in the cold-stressed fruit, indicating a general but differential intensified membrane peroxidation caused by temperature stress-induced ROS oxidation (Fig. 4f). Taken together, these results indicate that miR528 is likely the key regulator accounting for the change of ROS state in banana fruit, by modulating the *PPO* gene expression and subsequent PPO enzyme activity.

Conservation of miR528 in monocots

Recently, there have been several studies on the investigation of miR528 function. In rice, miR528 is involved in antiviral defense by targeting *L*-ascorbate oxidase (also called *L*-ascorbic acid oxidase) gene, thereby reducing the accumulation of ROS (Wu *et al.*, 2017). However, miR528 in maize affects lodging resistance by regulating the expression of two *LAC* genes (Sun *et al.*, 2018). Interestingly, here it was found that miR528 targets *PPO* genes in banana, another monocot species, and five of them bear a miR528 target site (alignment score ≤ 5) in the coding region near the 5' end (Fig. 5a). These findings suggest that the targeting preference of miR528 is likely to be species-specific and prompts

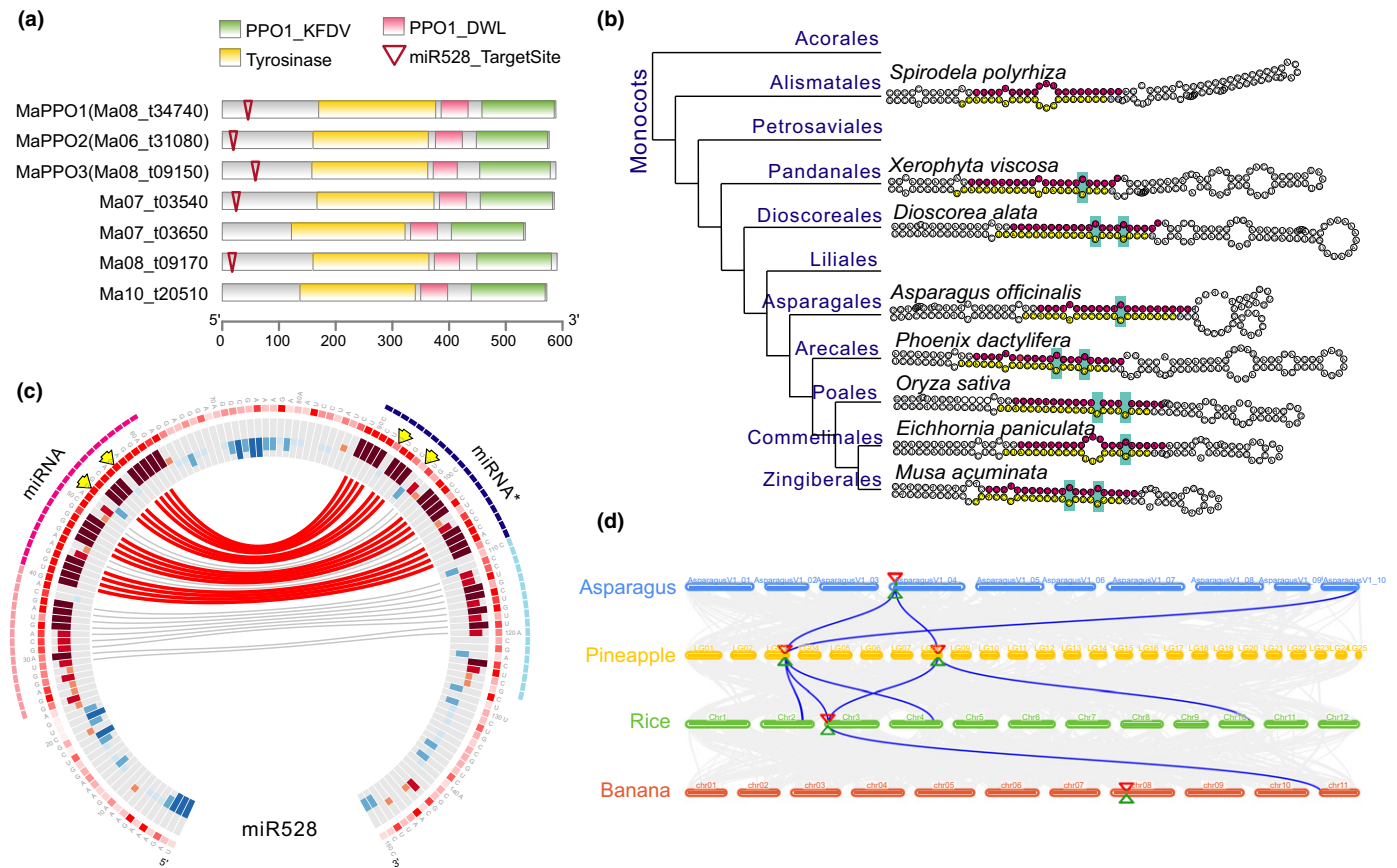


Fig. 5 Evolutionary conservation of copper-microRNA (miR528). (a) MiR528 targets five out of the seven *PPO* genes in banana. Rectangles denote protein sequences and conserved domains. Triangles show target sites of miR528 on *PPO*s in proteins coordinate. (b) Secondary structures of miR528 are conserved in monocots. Left panel, a dendrogram shows the evolutionary relationship of monocots basing on APG (Angiosperm Phylogeny Group) IV. Right panel, secondary structures of *MIR528* from representative species according to the dendrogram presented. Mature miR528 sequences are highlighted in pink whereas star sequences are highlighted in yellow. Conserved mismatches are denoted in red rectangles drawing with dash lines. (c) Sequences of miR528 are highly conserved among monocots. Purple, pink, dark-blue and light-blue bar on the most outside region denote miRNA region, region adjacent to miRNA, miRNA star region and region adjacent to miRNA star, respectively. Red bars indicate the possibility of bases to form double strand RNA, which are quantitatively indicated by the height of the bars. Curves refer to bases interacting with each other in the secondary structures of the precursors. Red lines refer to bases interacting 100% whereas gray lines show bases that interact in at least 50% of the species. (d) MiR528 is located in syntenic blocks in almost all monocots. Round rectangles denote chromosomes of four representative monocot species. Green triangles highlight *MIR528* loci whereas red triangles denote protein-coding genes adjacent to miR528 loci. All bezier curves connect protein-coding genes in syntenic blocks. Curves in blue are those gene pairs that include genes adjacent to *MIR528* loci. *PPO*, polyphenol oxidase.

exploration of the evolutionary history of miR528 and its targets in monocots. As reported previously (Liu *et al.*, 2005; Chen *et al.*, 2018b), miR528 is a miRNA restricted to the monocots. It likely emerged after the split of monocots from its common ancestor with eudicots, as no *MIR528* homologs was found in any eudicots or gymnosperms or basal angiosperms (i.e. *Amborella trichopoda*). By searching public sequence data, it was possible to trace the presence of *MIR528* as early as in duckweed (*Spirodela polyrhiza*), an aquatic species belonging to Alismatales (Fig. 5b). The *MIR528* precursors are highly conserved in both miRNA sequence and stem-loop structure (Fig. 5b), even positions of mismatches, the U-C mispairing at the 12th position (from the 5' end of miR528) and the G-G mispairing at the 16th position, are conserved in the miRNA/miRNA* duplex region (Fig. 5b,c). Moreover, alignment of miR528 precursor sequences revealed that the lower stem region below the miRNA/miRNA* duplex is of relatively high sequence similarity (Fig. 5c), a feature observed

recently for plant miRNAs processed by DCL1 (Chorostecki *et al.*, 2017; Xia *et al.*, 2017), suggesting that the miR528 hairpin precursor is processed in a base-to-loop manner. Synteny analysis showed that *MIR528* genes is located in a syntenic block which is conserved among many monocot genomes, for instance asparagus, pineapple and rice (Fig. 5d), but this syntenic relationship seems to be lost in banana as the banana *MIR528* gene is located in a chromosome different from the one containing the syntenic block (Fig. 5d). Taken together, all of these results indicated that miR528 is a genuine miRNA conserved in monocots.

miR528 targets a diverse set of genes encoding Cu-containing proteins

Given the fact that the currently validated miR528 targets varied greatly in different monocot plants, it seems that miR528 target genes, unlike most other miRNAs which usually maintain

conserved target relationship among different species, may undergo a high level of divergence. However, all of these validated target genes, *AAO* in rice, *LAC* in maize and *PPO* in banana, belong to the superfamily of genes encoding Cu-containing oxidases, containing 1–3 Cu centers. Both ascorbate oxidase and laccase have three Cu centers; polyphenol oxidase contains two Cu centers. To further uncover the diversity of miR528 target genes as completely as possible, a survey of miR528 target gene was performed using public plant genome data in combination with the OneKP data, which collected transcriptome data from as many as > 1000 plant species (Wickett *et al.*, 2014). This survey revealed that a wide range of different genes are potential targets of miR528, some of which seems to be present among distinct species, for instance, genes encoding callose synthases and granule-bound starch synthases (Table S4). Astonishingly, there are many Cu-containing protein encoding genes other than *PPO* and those reported before (*LAC* and *AAO*) serving as potential target genes of miR528, including monocopper proteins (plastocyanin, mavecyanin, uclacyanin), POD, SOD, amine oxidase (AO) and other multicopper proteins (Fig. 6a; Table S4). The cleavage of miR528 on *SOD* and *AO* genes was validated by

public degradome data (Fig. S4). For the overall targeting capacity of miR528 which was assessed by alignment scores (≤ 5), all of the genes encoding Cu-containing proteins seem to have good capacity for miR528 targeting, with the *POD* and *SOD* genes (Fig. 6a) largely having higher alignment scores of > 4. The location of the miR528 target site over the target genes was checked (Fig. 6b), showing that almost all are located out of the region encoding functional domains, and not in consistent positions (Fig. 6b). Position of target site varies even for the same type of genes; for instance, the target site can be either after or before the region encoding the Suf superfamily domain of ascorbate oxidases (Fig. 6b). In some cases, the miR528 target site is located at UTR regions in *PPO* or multicopper-oxidase genes (Fig. 6b). This location of target site in nonconserved sequence regions (UTR or beyond the functional domain region) and variation in position are likely the factors contributing to the great diversity of miR528 target genes. For these target genes, miR528 also show different target preferences (capacity) among different species (Fig. 6c). Overall, miR528 has evolved broader targets in Poales, with the genes encoding laccase, ascorbate oxidase and monocopper protein having better targeting capacity (lower

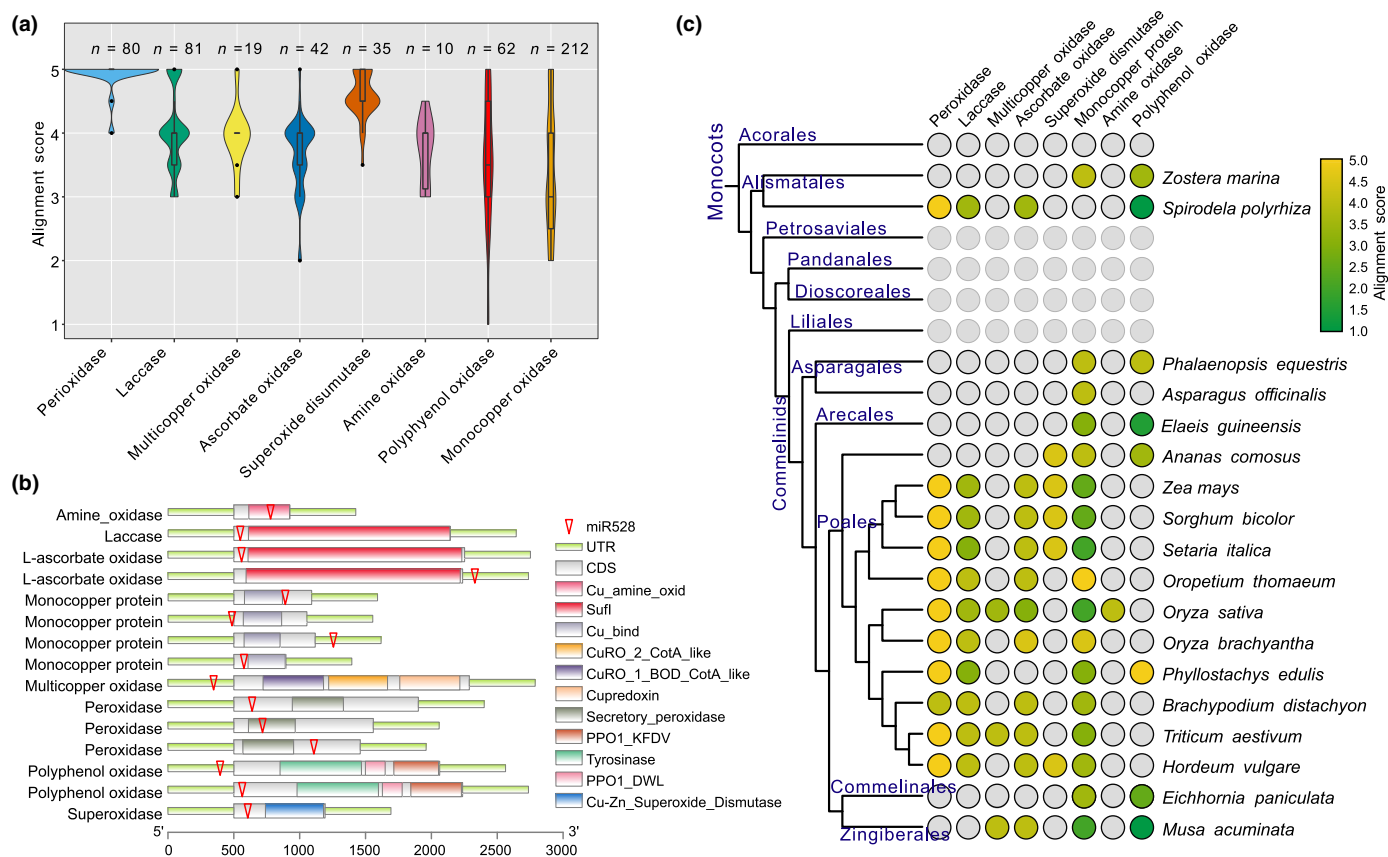


Fig. 6 Comparative analysis of copper (Cu)-microRNA (miR)528 targeting on genes encoding Cu-containing proteins. (a) MiR528 possesses good capacity for targeting genes of Cu-containing proteins. Texts above each bar denote numbers of genes belonging to each class of Cu-containing proteins. Only genes with alignment scores ≤ 5 were retained in violin plots. (b) Target sites of miR528 vary in position from gene to gene. miR528 has the potential to target genes in conserved domains, in coding regions other than conserved domains, and even in UTRs (untranslated regions). (c) Target preference of miR528 varies among different monocot plants. The dendrogram shows the evolutionary relationship of monocots basing on APG (Angiosperm Phylogeny Group) IV. Closed circles mean members of the corresponding gene family are targeted by miR528 in the specific species. The darker the color, the lower the alignment score.

alignment scores; Fig. 6c). The targeting of monocopper protein encoding genes is widely present in monocots, with almost all species studied possessing this regulation (Fig. 6c). By contrast, the miR528 targeting of *PPO* genes is probably restricted in non-Poales species (Fig. 6c). All of these results demonstrated that miR528 is a master regulator of genes encoding Cu-containing proteins, with diverse target preference, implying a dynamic evolutionary history of its target genes.

Subclasses of laccase genes are preferentially targeted by different miRNAs in land plants

Laccases are a class of Cu-containing proteins found in many plants, fungi and microorganisms. They possess various spatio-temporal functions (Solomon *et al.*, 1996), including the oxidative polymerization of lignin (Berthet *et al.*, 2011). The finding of the prevalence of miR528 targeting on laccase genes in Poales species suggesting miR528 is an important regulator of the expression of laccase genes. Apart from miR528, there are other miRNAs reported to regulate *LAC* genes as well, including miR397, miR408 and miR857 (also called Cu-miRNAs; Pilon, 2017). Among them, miR397 and miR408 are highly conserved among seed plants (Chen *et al.*, 2018b). The next question to ask

is how all of these miRNAs evolved to co-regulate the family of *LAC* genes in plants. To address this, phylogenetic analysis was performed for *LAC* genes using nine representative plant species and the targeting relationship of all these abovementioned miRNAs identified (Figs 7, S5). Largely consistent with previous reports (Turlapati *et al.*, 2011), the *LAC* gene family was separated into seven groups before the appearance of angiosperms (Fig. 7). All of the *LAC* groups are present in both eudicots and monocots, except the G6 group, which is likely restricted in eudicots. Regarding the miRNA targeting, each miRNAs shows preferential targeting of certain *LAC* groups. miR408, likely due to its wide presence in embryophyta (land plants), is the only miRNA targeting *LAC* genes in ancient land plants, including liverworts (*Marchantia polymorpha*) and mosses (*Physcomitrella patens*) (Fig. 7). Additionally, miR408 also targets *LAC* genes of the G3 group, which is rarely targeted by other miRNAs (Figs 7, S5). The miR397 targets almost all the members of the G1 and G2 *LAC* genes, and part of the G5 *LAC* genes (Figs 7, S5). Different from miR408 and miR397, the miR528 and miR857 target *LAC* genes dispersed in many groups, with only few members of a group retaining the miRNA target relationship, reflecting the restricted presence of these two miRNAs and possibly the rapid diversification of their target genes in plants.

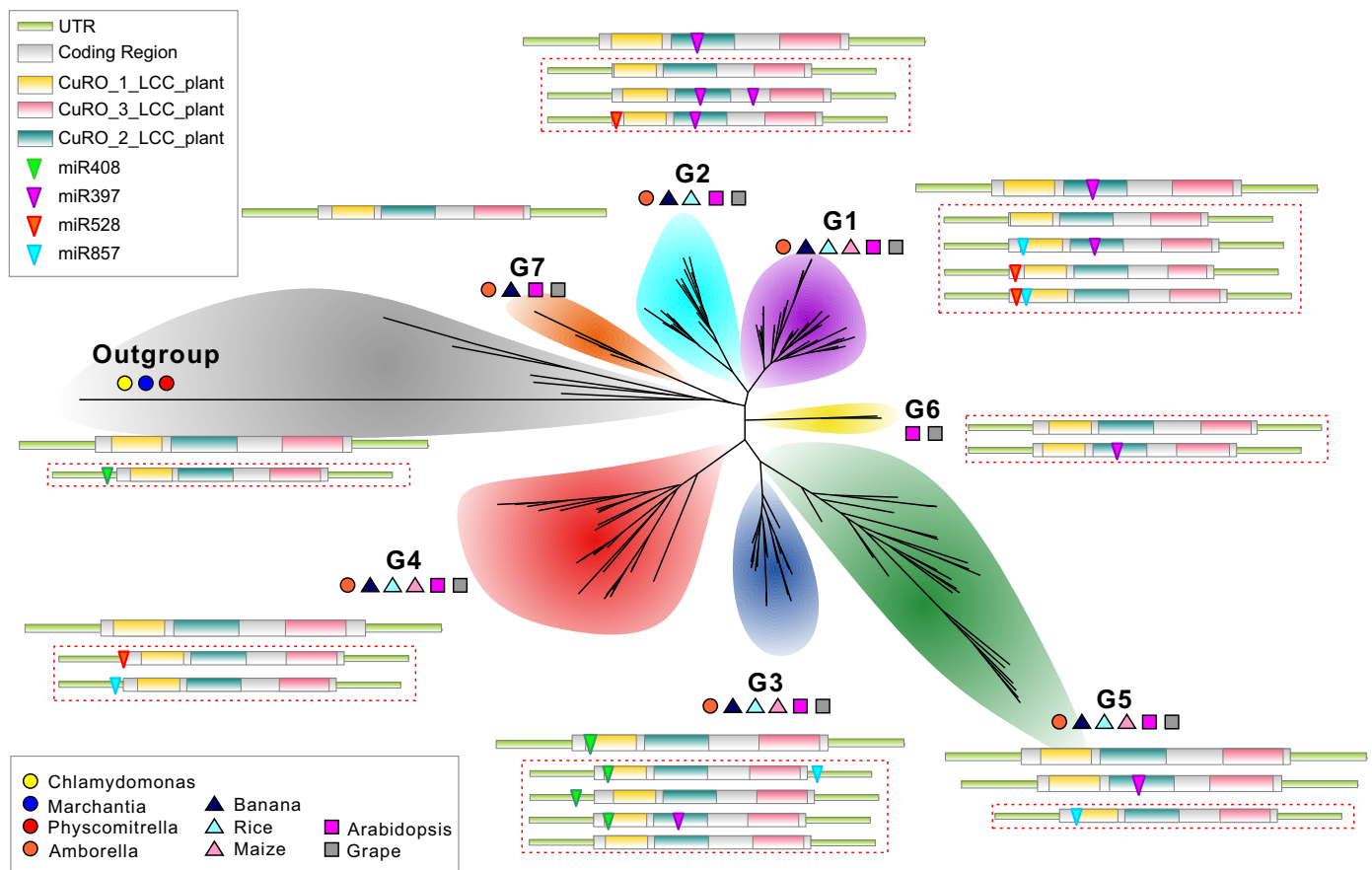


Fig. 7 Evolutionary history of targeting relationship between copper-microRNAs and laccases. An un-rooted tree is reconstructed for laccases from nine representative species with maximum-likelihood (ML) method using RAxML. All potential targeting patterns are presented. Major targeting patterns are shown above the minor patterns shown within red rectangles in dash lines.

Next the position of target sites along the *LAC* genes was checked, revealing that conserved miR408 and miR397 have target sites located within the sequence region encoding functionally important domains: the miR408 target site is located at the beginning of the region encoding the first cupredoxin domain (CuRO_1_LCC_plant) and miR397 site in the middle of the region encoding the second cupredoxin domain (CuRO_2_LCC_plant) (Figs 7, S5). The location of the miRNA target site within a sequence-conserved region (encoding a functional domain) explains well why these two miRNAs are capable of targeting a large number of *LAC* genes. By contrast, the target sites of miR528 and miR857 are located out of the region encoding functional domains, with miR528 target site at the beginning of *LAC* genes (before the region encoding the first cupredoxin domain) and miR857 site at either the beginning or the end of *LAC* genes (Figs 7, S5). In some cases, their target sites also are found in the 5'-UTR region of *LAC* genes (Fig. S5). Conceivably, this higher variation of target site distribution is caused by the higher sequence-changing ability of the nonconserved regions of *LAC* genes.

Discussion

MicroRNAs (miRNAs) are a class of important regulators in the plant responses to various abiotic stresses, including unfavorable temperature conditions. The miRNA-mediated cold stress response in plants has been reviewed recently (Megha *et al.*, 2018). The involvement in low temperature response has been demonstrated for a few copper (Cu)-miRNAs (i.e. miR408, miR397 and miR398) (Megha *et al.*, 2018). The present contribution explored banana miRNAs in response to temperature stresses, including both cold and heat, and it was demonstrated that miR528 plays a vital role in stress response by targeting a few polyphenol oxidase (*PPO* genes), which are the main contributors to the peel browning of banana fruit under cold stress. Comparative genomic analysis revealed that miR528, a monocot-specific miRNA, evolved with dynamic target preferences among different monocot species, but the majority of its target genes encode Cu-containing proteins, including a couple of well-known oxidases critical for cellular redox homeostasis.

miR528 targets *PPO* genes in banana

Previous studies have revealed the effects of temperature stress on plants and their response mechanisms. It is generally believed that temperature stress can rapidly alter membrane fluidity and/or integrity, changing the structure of different membrane proteins. Such changes could affect the function of the membrane-bound receptors/channels and initiate signal transduction reactions via phosphorylation and/or altered calcium fluxes (Horvath *et al.*, 1998). As a typical injury caused by low temperature stress that influences the postharvest quality of banana and most other fruits, tissue browning is believed to be the result of the redox homeostasis breakdown mainly manifested by membrane peroxidation caused by a reactive oxygen species (ROS) burst. In fact, browning is a consequence of oxidation of phenolic compounds

by *PPO* (Steffens *et al.*, 1994; Unal, 2005). In intact plant cells, phenolic compounds and *PPO* are located in vacuoles and plastids, respectively, whereas the cellular areas damaged by ROS upon stress allow the direct contact between *PPO* and phenolic compounds, triggering the enzymatic browning (Holderbaum *et al.*, 2010).

In the present study, it was shown that in banana, a group of Cu-miRNAs displayed differential response to temperature stresses and they jointly targeted a diverse set of redox enzyme genes encoding Cu-containing proteins. Among them, miR528 was revealed to play a leading role in banana, by negatively regulating its target *PPO* genes. It has a target site in five of the seven *PPO* genes in banana. In cold conditions, miR528 was diminished in abundance and the main target genes (*MaPPO1* and *MaPPO2*) were extremely upregulated, well over 100-fold (Figs 2a, 3c). *PPO* catalyzes the oxidation of phenolic compounds into highly reactive quinones, which subsequently interact with oxygen and proteins to generate ROS and brown complexes. Downregulation of miR528 in cold conditions caused the upsurge of *PPO* expression and subsequent high level of *PPO* activity, leading to the ROS burst and redox homeostasis breakdown. Thus, miR528-*PPO* probably plays a critical role in peel browning of banana fruit, which causes fruit quality deterioration and significant economic loss. In fact, the miR528-*PPO* regulatory module provides a good subject for biotechnological modification to obtain banana resources with better cold resistance. But this application requires an efficient banana genetic transformation system, which is currently lacking. Therefore, a

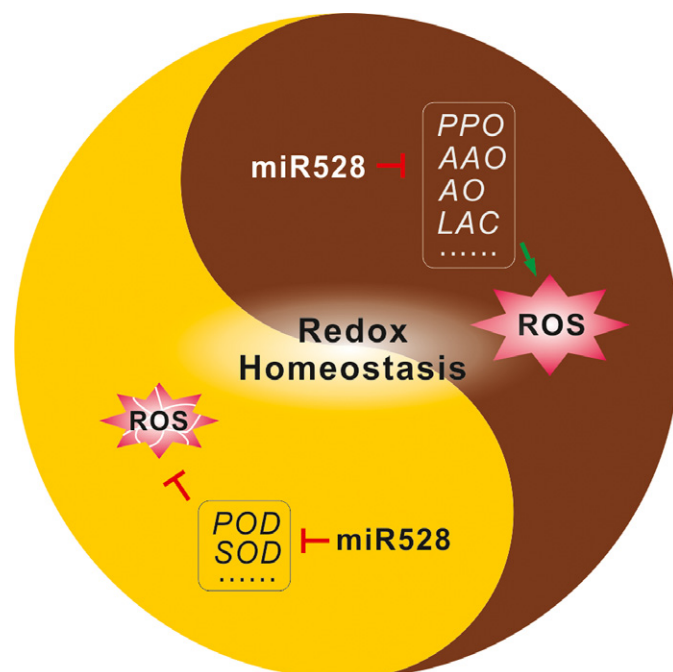


Fig. 8 Model for the role of copper-microRNA (miR)528 in cellular redox homeostasis. The 'Yin-Yang' symbol represents the balance of reactive oxygen species (ROS) level, contributed by miR528 roles in both ROS generation (by targeting *PPO*, polyphenol oxidase; *AAO*, ascorbate oxidase; *AO*, amine oxidase; *LAC*, laccase, etc.) and ROS scavenging (by *POD*, peroxidase; *SOD*, superoxide dismutase, etc.).

future focus will be on the transgenic system to manipulate miR528 expression in banana.

miR528 diversely regulates a set of genes encoding Cu-containing proteins in monocots

Polyphenol oxidase is a Cu-containing oxidase in a tetramer structure containing four Cu atoms per molecule, also referred to as tyrosinases (Vamos-Vigyazo, 1981; Mayer, 2006). By contrast to the targeting of *PPO* genes by miR528 in banana, it has been reported that miR528 targets an ascorbate oxidase (*AAO*) and two laccase (*LAC*) genes in rice and maize, respectively (Wu *et al.*, 2017; Sun *et al.*, 2018); these genes belong to multicopper oxidase as PPO. Similarly, in creeping bentgrass miR528 can target *AsAAO* and *AsCBPI* (encoding a Cu-containing protein) (Yuan *et al.*, 2015). In addition, miR528 has been demonstrated to target a few genes encoding monocopper proteins, like plastocyanin-like domain containing proteins (Zhou *et al.*, 2010). Intriguingly, the comprehensive comparative analysis herein identified many more genes that could be potentially targeted by miR528, and all of those genes with higher confidence (alignment score ≤ 4) encoded Cu-containing proteins with the miR528 target sites clearly differentiated (Fig. 5b). In other words, although its target preference diverged among different monocot species, it turns out that miR528 predominantly regulates relevant genes encoding Cu-containing proteins, which are involved in the process of tempering cellular redox homeostasis.

The present results uncovered that miR528, as a miRNA restricted to monocots, is able to target genes encoding Cu-containing proteins with all three types of Cu centers, for instance, plastocyanin and mavycyanin (Type I), superoxide dismutase (SOD) (Type II), PPO (Type III), and amine oxidase (AO), AAO and LAC (mixed types), in spite of distinct target preference among different species.

How did this broad and diverse target capacity of miR528 evolve? There are two possible explanations for this diversification. The first one might be the high diversification rate of genes encoding Cu-containing proteins. Evolutionary relationship inference based on increasing structural information for Cu-containing proteins, in combination with related sequence data, suggests that T2 Cu proteins appear to be derived from iron or manganese proteins, whereas T3 Cu proteins are believed to come from a simple mononuclear Cu ancestor, and trinuclear Cu oxidases with multiple T2 and T3 Cu centers are, in fact, unrelated to either T2 or T3 oxidases, but instead are derived from T1 mononuclear Cu proteins (Abolmaali *et al.*, 1998). This inferred evolutionary history of Cu-containing proteins agrees well with the observation that genes encoding monocopper proteins are more consistently regulated by miR528 compared to other classes (Fig. 5c). The other interpretation for the diversification of miR528 target genes is possibly the result of convergent evolution, as reflecting by the observation that target sites of miR528 are highly variable in position, even within the same gene family. In addition to normal oxygen metabolism, plants including monocots often are exposed to oxidative cellular environments that may result in the generation of toxic ROS, leading

to senescence and death of the organisms. Therefore, the control of redox state is critical for a plant's survival and the functional importance of miR528 in redox state control is possibly the exclusive driving force for a prospective convergent evolution process. Identification of potential target genes other than Cu-containing protein encoding genes further validated that miR528 is in a dynamic process of fast gain-and-loss of target genes.

miR528 is actively involved in the redox homeostasis in monocots

As a fundamental cell property, plant redox homeostasis controls ROS generation, senses deviation from and readjustment of the cellular redox state. All of these redox-related functions have been considered as decisive factors in plant stress acclimation and adaptation (Hossain & Dietz, 2016). Recent evidence shows that living plants can respond to some stress conditions as quickly as a few seconds (Kollist *et al.*, 2018). The present observation on the cold-stressed banana fruit also showed that the injury progressed very rapidly, with the symptom appearing within a few days (Fig. 1a). Some rapid responses are further shown to deliver throughout the entire plant via ROS and Ca^{2+} , possibly through the vascular system (Kollist *et al.*, 2018). ROS can be derived from the excitation of O_2 to form singlet oxygen ($^1\text{O}_2$) or from the reduction of O_2 to form stable ROS intermediates such as superoxide radical (O_2^-), hydrogen peroxide (H_2O_2) and hydroxyl radical ($\cdot\text{OH}$), in a stepwise manner. These ROS-generating reactions are catalyzed by various oxidases, among which multicopper-containing oxidases are a large class, including PPO, AAO, AAO and LAC (Mittler, 2002). In light, the chloroplasts and peroxisomes are the main ROS producers, whereas in darkness the mitochondria appear to be the main ROS production site (Moller *et al.*, 2007). To counteract ROS generation, plants also develop an enzymatic defense system including SOD, POD, CAT and other antioxidant enzymes, to eliminate free radicals, alleviate the membrane peroxidation and protect the membrane stability (Mittler, 2002). With the aggravation of stress, the oxidase system (ROS generating) exceeds the capacity of the antioxidant enzyme system (ROS scavenging), and excessively accumulating ROS may attack lipids, nucleic acids, proteins and chlorophyll through oxidation reactions, which eventually leads to the emergence of stress symptoms (like the peel browning of banana fruit under cold stress). Indeed, a network of ROS generation system, antioxidant defense system and redox sensors orchestrates the plant redox homeostasis, which serves as a critical integrator of environmental changes to control growth and stress responses (Dietz, 2008; Foyer & Noctor, 2009; Gill & Tuteja, 2010).

It was found herein that miR528 is capable of targeting myriad genes encoding Cu-containing proteins, including both the ROS-generating oxidases (PPO, AAO, AO, LAC) and the antioxidant ROS-scavenging enzymes (POD, SOD). This suggests that miR528 probably exerts dual roles (ROS generating and ROS scavenging) in ROS metabolism, essential for cellular redox homeostasis (Fig. 8). However, the dual roles of miR528 are not equally maintained in each monocot species. Generally, miR528 regulates genes important for ROS generation, implying a more

important role of this miRNA in ROS-scavenging. As the targeting efficacy of miR528 on different target genes was assessed solely by the pairing score, which may misestimate the real strength of miRNA mediated silencing effects at both transcriptional level (mRNA cleavage) and post-transcriptional level (protein translation inhibition), it is possible that the role of miR528 might be variable among different species, or even under different conditions within the same species.

Acknowledgements

This work was supported by awards from the National Natural Science Foundation of China (31772371, 31872063 and 31301822); National Key Technology R&D Program of China (2017YFD0401301); Natural Science Foundation of Guangdong Province (2015A030313686); the Innovation Team Project of the Department of Education of Guangdong Province (2016KCXTD011). We thank Dr Uciel Chorostecki and Dr Javier F. Palatnik from Universidad Nacional de Rosario (Rosario 2000, Argentina) for sharing the codes for preparing the Circos plot. We are grateful to Dr Blake C. Meyers for the critical reading of the manuscript. Support from National Botanical Gardens, Chinese Academy of Sciences is appreciated.

Author contributions

HZ, YJ, XD and RX conceived the study and designed the experiments; HZ, CC and RX performed most of the data analyses; JZ and ZY collected samples and measured physiological parameters; HZ, JZ and YL performed 5' RACE and sRNA Northern blotting; HZ, CC and RX prepared the figures and wrote the manuscript; HQ, YJ and XD provided input and revised the manuscript; and HZ and CC contributed equally to this work.

ORCID

Chengjie Chen  <https://orcid.org/0000-0001-5964-604X>
 Xuewu Duan  <https://orcid.org/0000-0002-9621-3865>
 Yueming Jiang  <https://orcid.org/0000-0002-4648-9572>
 Rui Xia  <https://orcid.org/0000-0003-2409-1181>
 Jun Zeng  <https://orcid.org/0000-0002-8478-4556>
 Hong Zhu  <https://orcid.org/0000-0002-5555-1227>
 Hongxia Qu  <https://orcid.org/0000-0003-1930-8526>

References

- Abdel-Ghany SE, Pilon M. 2008. MicroRNA-mediated systemic down-regulation of copper protein expression in response to low copper availability in *Arabidopsis*. *Journal of Biological Chemistry* **283**: 15932–15945.
- Abolmaali B, Taylor HV, Weser U. 1998. Evolutionary aspects of copper containing centers in copper proteins. *Structure and Bonding* **91**: 91–190.
- Akter S, Huang J, Waszczak C, Jacques S, Gevaert K, Van Breusegem F, Messens J. 2015. Cysteines under ROS attack in plants: a proteomics view. *Journal of Experimental Botany* **66**: 2935–2944.
- Berthet S, Demont-Caulet N, Pollet B, Bidzinski P, Cezard L, Le Bris P, Borrega N, Herve J, Blondet E, Balzergue S *et al.* 2011. Disruption of *LACCASE4* and 17 results in tissue-specific alterations to lignification of *Arabidopsis thaliana* stems. *Plant Cell* **23**: 1124–1137.
- Burkhead JL, Reynolds KA, Abdel-Ghany SE, Cohu CM, Pilon M. 2009. Copper homeostasis. *New Phytologist* **182**: 799–816.
- Chavez-Hernandez EC, Alejandri-Ramirez ND, Juarez-Gonzalez VT, Dinkova TD. 2015. Maize miRNA and target regulation in response to hormone depletion and light exposure during somatic embryogenesis. *Frontiers in Plant Science* **6**: 555.
- Chen C, Xia R, Chen H, He Y. 2018a. TBtools, a toolkit for biologists integrating various HTS-data handling tools with a user-friendly interface. *bioRxiv*. doi: 10.1101/289660.
- Chen C, Zeng Z, Liu Z, Xia R. 2018b. Small RNAs, emerging regulators critical for the development of horticultural traits. *Horticulture Research* **5**: 63.
- Chen X. 2012. Small RNAs in development – insights from plants. *Current Opinion in Genetics & Development* **22**: 361–367.
- Choi M, Davidson VL. 2011. Cupredoxins—a study of how proteins may evolve to use metals for bioenergetic processes. *Metallomics* **3**: 140–151.
- Chorostecki U, Moro B, Rojas AML, Debernardi JM, Schapire AL, Notredame C, Palatnik JF. 2017. Evolutionary footprints reveal insights into plant microRNA biogenesis. *Plant Cell* **29**: 1248–1261.
- Dietz KJ. 2008. Redox signal integration: from stimulus to networks and genes. *Physiologia Plantarum* **133**: 459–468.
- Dugas DV, Bartel B. 2008. Sucrose induction of *Arabidopsis* miR398 represses two Cu/Zn superoxide dismutases. *Plant Molecular Biology* **67**: 403–417.
- Foyer CH, Noctor G. 2009. Redox regulation in photosynthetic organisms: signaling, acclimation, and practical implications. *Antioxidants & Redox Signaling* **11**: 861–905.
- Gill SS, Tuteja N. 2010. Reactive oxygen species and antioxidant machinery in abiotic stress tolerance in crop plants. *Plant Physiology and Biochemistry* **48**: 909–930.
- Higashi Y, Takechi K, Takano H, Takio S. 2013. Involvement of microRNA in copper deficiency-induced repression of chloroplastic CuZn-superoxide dismutase genes in the moss *Physcomitrella patens*. *Plant and Cell Physiology* **54**: 1345–1355.
- Holderbaum DF, Kon T, Kudo T, Guerra MP. 2010. Enzymatic browning, polyphenol oxidase activity, and polyphenols in four apple cultivars: dynamics during fruit development. *HortScience* **45**: 1150–1154.
- Horvath I, Glatz A, Varvasovszki V, Torok Z, Pali T, Balogh G, Kovacs E, Nadasdi L, Benko S, Joo F *et al.* 1998. Membrane physical state controls the signaling mechanism of the heat shock response in *Synechocystis* PCC 6803: identification of *hsp17* as a “fluidity gene”. *Proceedings of the National Academy of Sciences, USA* **95**: 3513–3518.
- Hossain MS, Dietz KJ. 2016. Tuning of redox regulatory mechanisms, reactive oxygen species and redox homeostasis under salinity Stress. *Frontiers in Plant Science* **7**: 548.
- Jones-Rhoades MW, Bartel DP, Bartel B. 2006. MicroRNAs and their regulatory roles in plants. *Annual Review of Plant Biology* **57**: 19–53.
- Knight MR, Knight H. 2012. Low-temperature perception leading to gene expression and cold tolerance in higher plants. *New Phytologist* **195**: 737–751.
- Kollist H, Zandalinas SI, Sengupta S, Nuhkat M, Kangasjarvi J, Mittler R. 2018. Rapid responses to abiotic stress: priming the landscape for the signal transduction network. *Trends in Plant Science* **24**: 25–37.
- Kotchoi SO, Gachomo EW. 2006. The reactive oxygen species network pathways: an essential prerequisite for perception of pathogen attack and the acquired disease resistance in plants. *Journal of Biosciences* **31**: 389–404.
- Kovtun Y, Chiu WL, Tena G, Sheen J. 2000. Functional analysis of oxidative stress-activated mitogen-activated protein kinase cascade in plants. *Proceedings of the National Academy of Sciences, USA* **97**: 2940–2945.
- Li T, Li H, Zhang YX, Liu JY. 2011. Identification and analysis of seven H₂O₂-responsive miRNAs and 32 new miRNAs in the seedlings of rice (*Oryza sativa* L. ssp. *indica*). *Nucleic Acids Research* **39**: 2821–2833.
- Li Y, Zhang Y, Shi D, Liu X, Qin J, Ge Q, Xu L, Pan X, Li W, Zhu Y *et al.* 2013. Spatial-temporal analysis of zinc homeostasis reveals the response mechanisms to acute zinc deficiency in *Sorghum bicolor*. *New Phytologist* **200**: 1102–1115.
- Liu B, Li P, Li X, Liu C, Cao S, Chu C, Cao X. 2005. Loss of function of *OsDCL1* affects microRNA accumulation and causes developmental defects in rice. *Plant Physiology* **139**: 296–305.
- Lu S, Yang C, Chiang VL. 2011. Conservation and diversity of microRNA-associated copper-regulatory networks in *Populus trichocarpa*. *Journal of Integrative Plant Biology* **53**: 879–891.

- Matasci N, Hung LH, Yan Z, Carpenter EJ, Wickett NJ, Mirarab S, Nguyen N, Warnow T, Ayyampalayam S, Barker M *et al.* 2014. Data access for the 1,000 Plants (1KP) project. *Gigascience* 3: 17.
- Mayer AM. 2006. Polyphenol oxidases in plants and fungi: going places? A review. *Phytochemistry* 67: 2318–2331.
- Megha S, Basu U, Kav NNV. 2018. Regulation of low temperature stress in plants by microRNAs. *Plant, Cell & Environment* 41: 1–15.
- Miller G, Schlauch K, Tam R, Cortes D, Torres MA, Shulaev V, Dangl JL, Mittler R. 2009. The plant NADPH oxidase RBOHD mediates rapid systemic signaling in response to diverse stimuli. *Science Signaling* 2: ra45.
- Mittler R. 2002. Oxidative stress, antioxidants and stress tolerance. *Trends in Plant Science* 7: 405–410.
- Mittler R, Vanderauwera S, Suzuki N, Miller G, Tognetti VB, Vandepoele K, Gollery M, Shulaev V, Van Breusegem F. 2011. ROS signaling: the new wave? *Trends in Plant Science* 16: 300–309.
- Moller IM, Jensen PE, Hansson A. 2007. Oxidative modifications to cellular components in plants. *Annual Review of Plant Biology* 58: 459–481.
- Nakamura K, Go N. 2005. Function and molecular evolution of multicopper blue proteins. *Cellular and Molecular Life Sciences* 62: 2050–2066.
- Noctor G, Mhamdi A, Foyer CH. 2014. The roles of reactive oxygen metabolism in drought: not so cut and dried. *Plant Physiology* 164: 1636–1648.
- Orozco-Cardenas M, Ryan CA. 1999. Hydrogen peroxide is generated systemically in plant leaves by wounding and systemin via the octadecanoid pathway. *Proceedings of the National Academy of Sciences, USA* 96: 6553–6557.
- Petrov VD, Van Breusegem F. 2012. Hydrogen peroxide—a central hub for information flow in plant cells. *AoB Plants* 2012: pls014.
- Pilon M. 2017. The copper microRNAs. *New Phytologist* 213: 1030–1035.
- Ragupathy R, Ravichandran S, Mahdi MS, Huang D, Reimer E, Domaratzki M, Cloutier S. 2016. Deep sequencing of wheat sRNA transcriptome reveals distinct temporal expression pattern of miRNAs in response to heat, light and UV. *Scientific Reports* 6: 39373.
- Ramachandran V, Chen X. 2008. Small RNA metabolism in *Arabidopsis*. *Trends in Plant Science* 13: 368–374.
- Sharma D, Tiwari M, Lakhwani D, Tripathi RD, Trivedi PK. 2015. Differential expression of microRNAs by arsenate and arsenite stress in natural accessions of rice. *Metallomics* 7: 174–187.
- Solomon EI, Sundaram UM, Machonkin TE. 1996. Multicopper oxidases and oxygenases. *Chemical Reviews* 96: 2563–2605.
- Stamatakis A. 2014. RAxML version 8: a tool for phylogenetic analysis and post-analysis of large phylogenies. *Bioinformatics* 30: 1312–1313.
- Steffens JC, Harel E, Hunt MD. 1994. Polyphenol oxidase. In: Ellis BE, Kuroki GW, Stafford HA, eds. *Genetic engineering of plant secondary metabolism*. New York, NY, USA: Plenum Publishing, 275–312.
- Sun Q, Liu X, Yang J, Liu W, Du Q, Wang H, Fu C, Li WX. 2018. MicroRNA528 affects lodging resistance of maize by regulating lignin biosynthesis under nitrogen-luxury conditions. *Molecular Plant* 11: 806–814.
- Sunkar R, Kapoor A, Zhu JK. 2006. Posttranscriptional induction of two Cu/Zn superoxide dismutase genes in *Arabidopsis* is mediated by downregulation of miR398 and important for oxidative stress tolerance. *Plant Cell* 18: 2051–2065.
- Sunkar R, Li YF, Jagadeeswaran G. 2012. Functions of microRNAs in plant stress responses. *Trends in Plant Science* 17: 196–203.
- Turlapati PV, Kim KW, Davin LB, Lewis NG. 2011. The laccase multigene family in *Arabidopsis thaliana*: towards addressing the mystery of their gene function(s). *Planta* 233: 439–470.
- Unal MU. 2005. Properties of polyphenol oxidase from Anamur banana (*Musa cavendishii*). *Food Chemistry* 100: 909–913.
- Vamos-Vigyazo L. 1981. Polyphenol oxidase and peroxidase in fruits and vegetables. *Critical Reviews in Food Science and Nutrition* 15: 49–127.
- Voynet O. 2009. Origin, biogenesis, and activity of plant microRNAs. *Cell* 136: 669–687.
- Wahid A, Gelani S, Ashraf M, Foolad MR. 2007. Heat tolerance in plants: an overview. *Environmental & Experimental Botany* 61: 199–223.
- Wickett NJ, Mirarab S, Nguyen N, Warnow T, Carpenter E, Matasci N, Ayyampalayam S, Barker MS, Burleigh JG, Gitzendanner MA *et al.* 2014. Phylotranscriptomic analysis of the origin and early diversification of land plants. *Proceedings of the National Academy of Sciences, USA* 111: E4859–E4868.
- Wu J, Yang R, Yang Z, Yao S, Zhao S, Wang Y, Li P, Song X, Jin L, Zhou T *et al.* 2017. ROS accumulation and antiviral defence control by microRNA528 in rice. *Nature Plants* 3: 16203.
- Xia R, Xu J, Meyers BC. 2017. The Emergence, evolution, and diversification of the miR390-TAS3-ARF pathway in land Plants. *Plant Cell* 29: 1232–1247.
- Xia XJ, Zhou YH, Shi K, Zhou J, Foyer CH, Yu JQ. 2015. Interplay between reactive oxygen species and hormones in the control of plant development and stress tolerance. *Journal of Experimental Botany* 66: 2839–2856.
- Yamasaki H, Abdel-Ghany SE, Cohu CM, Kobayashi Y, Shikanai T, Pilon M. 2007. Regulation of copper homeostasis by micro-RNA in *Arabidopsis*. *Journal of Biological Chemistry* 282: 16369–16378.
- Yan H, Saika H, Maekawa M, Takamura I, Tsutsumi N, Kyojuka J, Nakazono M. 2007. Rice tillering dwarf mutant *dwarf3* has increased leaf longevity during darkness-induced senescence or hydrogen peroxide-induced cell death. *Genes & Genetic Systems* 82: 361–366.
- Yuan S, Li Z, Li D, Yuan N, Hu Q, Luo H. 2015. Constitutive expression of rice microRNA528 alters plant development and enhances tolerance to salinity stress and nitrogen starvation in creeping bentgrass. *Plant Physiology* 169: 576–593.
- Zhou M, Gu L, Li P, Song X, Wei L, Chen Z, Cao X. 2010. Degradome sequencing reveals endogenous small RNA targets in rice (*Oryza sativa* L. ssp. indica). *Frontiers in Biology* 5: 67–90.

Supporting Information

Additional Supporting Information may be found online in the Supporting Information section at the end of the article.

Fig. S1 Differentially expressed miRNAs identified from sRNA-seq and experimental validation.

Fig. S2 Target validation of selected miRNAs.

Fig. S3 Expression analysis of miRNAs and target genes in response to temperature stresses.

Fig. S4 Position variation of miR528 target site in different target genes.

Fig. S5 Phylogenetic relationship of laccases from selective plant species (A complete figure for Fig. 7).

Table S1 Probes for RNA gel blot and primers for real-time qPCR and RLM-5'-RACE.

Table S2 Differentially expressed miRNAs under temperature stresses in banana.

Table S3 All predicted target genes of temperature-responsive miRNAs in banana.

Table S4 Potential miR528 targets in monocots.

Please note: Wiley Blackwell are not responsible for the content or functionality of any Supporting Information supplied by the authors. Any queries (other than missing material) should be directed to the *New Phytologist* Central Office.